the plant journal

SEB Society for Experimental Biology

The Plant Journal (2012) **70**, 147–156 doi: 10.1111/j.1365-313X.2012.04931.x

HIGH-RESOLUTION MEASUREMENTS IN PLANT BIOLOGY

The structure of the phloem – still more questions than answers

Michael Knoblauch[1,*] and Karl Oparka[2]

[1]*School of Biological Sciences, Washington State University, Pullman, WA, USA, and*

[2]*Institute of Molecular Plant Sciences, University of Edinburgh, Edinburgh, UK*

Received 2 November 2011; revised 27 January 2012; accepted 31 January 2012.

*For correspondence (e-mail knoblauch@wsu.edu).

SUMMARY

Long-distance assimilate distribution in higher plants takes place in the enucleate sieve-tube system of the phloem. It is generally accepted that flow of assimilates is driven by an osmotically generated pressure differential, as proposed by Ernst Münch more than 80 years ago. In the period between 1960 and 1980, the pressure flow hypothesis was challenged when electron microscopic images suggested that sieve tubes contain obstructions that would prevent passive flow. This led to the proposal of alternative translocation mechanisms. However, most investigators came to the conclusion that obstructions in the sieve-tube path were due to preparation artifacts. New developments in bioimaging have vastly enhanced our ability to study the phloem. Unexpectedly, *in vivo* studies challenge the pressure-flow hypothesis once again. In this review we summarize current investigations of phloem structure and function and discuss their impact on our understanding of long-distance transport in the phloem.

Keywords: phloem, sieve elements, long distance transport, Münch's pressure flow hypothesis, high resolution imaging, forisomes, microscopy rhizosphere chambers.

INTRODUCTION

The evolution of land plants led to larger size and complexity of the plant body, which in turn increased the demands for long distance assimilate and signal transport. Vascular tissues evolved into two effective microfluidics systems with different tasks. The xylem is a network of channels that consists of dead cells that translocate water and nutrients through the apoplast. The transport of assimilates, on the other hand, occurs in the phloem, a tissue that contains living cells called sieve elements. Consecutive, interconnected files of sieve elements form sieve tubes that are functionally supported by companion cells and phloem parenchyma. In contrast to the xylem, sieve tubes of the phloem translocate fluids in the symplasm. Frictional interactions with cell ingredients define the resistance of the sieve-tube system, and so it is not surprising to observe a consecutive increase of organelle removal within sieve elements during land plant evolution. While sieve element precursors in mosses contain most of the organelles typical for plant cells, angiosperm sieve elements lost most of them when they mature, with the exception of mitochondria, sieve element plastids, ER and phloem proteins (P-proteins) (Behnke and Sjolund, 1990; Van Bel and Knoblauch, 2000). The minimal organelle repertoire of sieve elements is not sufficient for self-supported survival. Instead, companion cells, ontogenetically derived from the same mother cell, support the sieve elements and appear to be critical for sieve-tube function (Oparka and Turgeon, 1999).

Why is the structure of the sieve element important?

While it is clear that a reduction in organelles went hand-in-hand with the development of pipes for solute flow, the nature and location of the remaining organelles remains a matter of considerable debate. For solutes to move unimpeded through sieve elements would require that the remaining organelles are located in such a way that their effect on overall resistance is minimal. The exact distribution of sieve-element contents has been hotly debated for the last century. Light microscopy studies depicted sieve elements

to containing 'P-protein' plugs (Hartig, 1854), callose, and/or inclusions released from plastids (Barclay *et al.*, 1977). This led to a view, inconsistent with radiolabel-based translocation studies, that sieve elements might be naturally occluded in the 'translocating state' (Fensom, 1957; Spanner, 1958). One of the main problems is that sieve-elements are remarkably sensitive to damage because of the enormously high turgor pressures they generate. Severing the sieve-tube system leads to surge artifacts as turgor pressure is lost and organelles become displaced, blocking the sieve plates and the specialized plasmodesmata that connect the sieve element and companion cell (Oparka and Turgeon, 1999). Less invasive approaches for studying sieve-element structure (Knoblauch and van Bel, 1998), however, depict the sieve element as a pipe relatively free from obstruction until damage or turgor loss occurs. However, it is still not clear how the remaining sieve element contents affect flow through pipes of remarkably small diameters in the range of 2–50 μm. Such precise structural data are crucial to estimate frictional interactions of the fluid with the tube.

Historical context

Since translocation velocities were measured to be in the range of 200–400 μm s^{-1} (Canny, 1975; Windt *et al.*, 2006), diffusion and cytoplasmic streaming were discarded as potential translocation mechanisms. Bright-field observations of sieve elements suggested the presence of 'transcellular strands' inside the sieve-tube lumen (Thaine, 1961). Initially the strands were regarded as being surrounded by membranes (Thaine, 1962). Since there was no evidence found for membranes in TEM investigations, the strands were thought to be endoplasmic tubules composed of P-proteins, driving phloem flow by the production of peristaltic waves (Thaine, 1969). Later it was shown that the presence of strands in sieve tubes could be traced back to preparation artifacts (Evert *et al.*, 1973; Johnson *et al.*, 1976; Knoblauch and van Bel, 1998). The two most discussed potential modes of translocation were the electro-osmotic theory (Fensom, 1957; Spanner, 1958, 1970) and the pressure-flow hypothesis (Münch, 1927, 1930). The electro-osmotic theory required sieve plate pores to be filled with material. Potassium pumps were suggested to generate a circulation of ions through the plate. The ions would then flow back through the apoplast after release from the sieve tube. This circulation would polarize the plate and cause an electro-osmotic flow of assimilates. In fact, most electron micrographs showed pores occluded by P-proteins. On the other hand, open pores and a relatively unobstructed lumen were required for the pressure flow hypothesis, since friction has to be relatively low to allow passive flow driven by a pressure gradient. Although only a low percentage of micrographs revealed open pores and an unobstructed lumen, most investigators supported the pressure-flow hypothesis and argued that obstructions were due to surge artifacts. Nowadays, very few researchers question the pressure-flow hypothesis, and it is taught to undergraduate students as the driving force for solute flow in the phloem. However, to this date, the pressure flow hypothesis rests more on its plausibility than on experimental proof (Knoblauch and Peters, 2010).

With this background in mind, we will discuss various techniques that hold potential in elucidating the structure of sieve tubes in relation to their function. Recent developments have led to surprising results and it appears that it may be necessary to reassess our current views of phloem translocation.

NEW DEVELOPMENTS IN PHLOEM IMAGING

There are two events that lead to major advances in bioimaging. One is the development of new instrumentation that has had a broad impact on the scientific community generally. The other is the development of new protocols designed to investigate specific cells or tissues. Both are equally important for advancing the field, and are the basis for the discussion in the following section.

Bright field microscopy

One of the biggest problems facing phloem research is that in contrast to other cell types, sieve elements form a symplasmic continuum of relatively low resistance between individual sieve-element members. Because sieve tubes are surrounded by several cells, preparation is required for visualization which most often leads to injury of the tube system. Therefore, it is difficult to tell which structures are artifacts and which ones resemble the *in vivo* state, not helped by the fact that sieve elements are one of the smallest cell types in the plant body.

Initial observations of the phloem utilized light microscopy (Hartig, 1854). Due to the low contrast and the small size of the structures present in sieve tubes, investigations on sieve tube components were limited. The general cell anatomy, however, was intensively studied and recognized as crucial to determining the mechanism of translocation (Esau and Cheadle, 1959). Important parameters to estimate flow in the tube system are the length and radius of sieve elements, and the length, radius, and number of pores per sieve plate (Thompson, 2006). Measurement of sieve-element parameters is theoretically possible by bright field microscopy, but sieve-plate values such as pore diameters are difficult to obtain (Figure 1a).

The length/radius ratio of sieve elements is usually in the range between 10 and 100 (see table 3 in Thompson and Holbrook, 2003; Mullendore *et al.*, 2010). One effective way to decrease friction in the tube system is to increase the diameter of the tube. Large tube diameters of 50 μm and more are typical for Cucurbitaceae. The aspect ratio (length/radius ratio) is low, however, usually in the range of 10. Another strategy to reduce friction is to reduce the number of sieve plates in the tube system, leading to elongated sieve

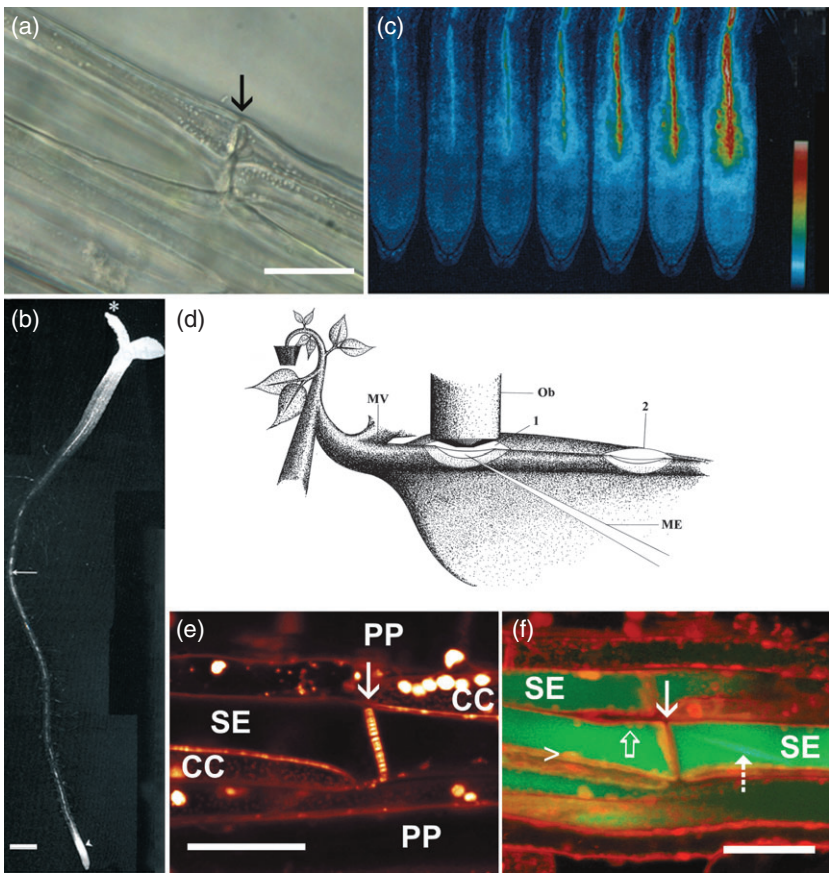

Figure 1. Microscopy of sieve tubes.
(a) Bright field micrograph of a Nicotiana benthamiana sieve tube. A sieve plate (arrow) separates two sieve elements. While the resolution is sufficient to measure sieve element length and diameter, sieve plate, and especially sieve plate pores are too small to allow accurate measurements.
(b) Phloem transport of carboxyfluorescein (CF) in an intact Arabidopsis seedling. The dye was applied to a single cotyledon (*) and became loaded into the phloem where it moved to the opposite cotyledon, hypocotyl and root. Within the root the two phloem poles are visible (arrow) and undergo considerable twisting. Near the root apex the dye is unloaded into a discrete zone surrounding the protophloem.
(c) Time series showing phloem unloading in the root tip of an Arabidopsis seedling. From the protophloem sieve elements the dye spreads symplasmically outwards into surrounding tissues. The images were taken at 6 min intervals, and the root tip extended 60 μm during the observation period. Figures b and c are from Oparka *et al.* (1994) with permission of the publisher.
(d) Sketch of preparation for observation of intact phloem. Cortical cell layers are removed from the main vein (MV) of a leaf to produce an observation window (1). Sieve tubes are observed with a water immersion objective (Ob) that is dipped directly into the bathing medium. A second window is cut upstream (2) and phloem mobile fluorescent dyes are applied. The dyes are translocated downstream where they eventually reach the site of observation. Fluorescence allows high resolution imaging by confocal microscopy and provides proof that the observed sieve tubes are actively translocating. Microcapillaries (ME) allow manipulation and measurements on intact tubes.
(e, f) Confocal images of intact sieve tubes in Vicia faba.
(e) Sieve plate area after staining with the membrane selective dye Rh-160. The sieve plate (arrow) containing numerous pores separates two sieve elements (SE). Surrounding companion cells (CC) and phloem parenchyma cells (PP) are well visible.
(f) Confocal micrograph of sieve elements (SE) stained with distantly applied and translocated HPTSA (green) and locally applied Rh-160. Sieve tube components such as sieve plate (closed arrow), parietal proteins (arrowhead), SE-plastids (open arrow) and forisomes (dashed arrow) are visible. Figures d–f are from Knoblauch and van Bel (1998) with permission of the publisher.
 Bars: a = 30 μm; b = 500 μm; e, f = 20 μm.

elements of 1mm lengths and more, which can be found in many grasses. Here, the aspect ratio is often close to 100. There is however, no clear, general evolutionary trend discernible. Length and diameter, as well as length/diameter ratios may vary significantly between species of the same family, genus, or even within the same plant, depending on environmental conditions. Thus, a generalization is difficult (but see Jensen *et al.*, 2011).

Concerning geometrical parameters of the sieve plate, Esau and Cheadle (1959) conducted a systematic light microscopic investigation. They measured pore diameters and pore numbers in 160 dicot species from 129 genera and 60 families. Unfortunately, they averaged the values from all species and only compared average values between simple and compound plates. Raw data for species-specific pore parameters were not provided. However, they pointed out

that the actual pore opening was in most cases below the resolution limit, a fact that caused major problems for phloem flow modeling for many decades (Thompson and Holbrook, 2003; Thompson, 2005, 2006). Precise measurements of sieve tubes and of sieve-plate geometry became available only recently using scanning electron microscopy (SEM; see below).

Confocal laser scanning microscopy (CLSM)

Within the last 15 years, confocal microscopy has developed into one of the most important microscopic tools available for cell biologists. Although, as with all forms of light microscopy, the resolution of CLSM is finite due to the diffraction limit imposed by the wavelength of light (but see super resolution microscopy below), it allows non-invasive imaging and 3D reconstructions of living cells and tissues. Although offering a significant advance upon the prevailing imaging technology, the popularity of CLSM undoubtedly owed a great deal to the development of fluorescent proteins as genetic tags and the subsequent generation of transgenic plants expressing fusion proteins constitutively allowing *in vivo* investigations into protein action and location in subcellular compartments. However, it has proven difficult until very recently to target fluorescent proteins specifically to sieve-element components.

The combination of laser excitation and point scanning facilitates imaging with greater resolution at greater depths, which is of specific advantage for phloem investigations. In addition, specific staining and the elimination of out-of-focus background light allows high-quality imaging at the limits of diffraction. A notable investigation was performed by Schulz (1992) who observed significant ER clusters on sieve plates and inside sieve-plate pores of living conifer phloem in bark strips. The first study to examine phloem translocation *in vivo* was conducted by Oparka *et al.* (1994). Here, small *Arabidopsis* seedlings growing on agar within petri dishes were labeled with the phloem-mobile dye, carboxyfluorescein (CF). This dye is interesting because it possesses a unique combination of membrane permeability and dissociation constant that make it similar to the phloem-mobile herbicide, glyphosate (Grignon *et al.*, 1989), allowing it be visualised in sieve tubes and also during its unloading from the phloem. (Figure 1b,c). In a series of studies, Wright and Oparka (1994, 1996; Wright *et al.*, 1996) examined the phloem transport of a range of fluorescent probes that differed in their physicochemical properties. As a general rule, there was a strong correlation between the dye's physicochemical properties and its predicted phloem mobility, although there were some notable exceptions (Wright and Oparka, 1994; Wright *et al.*, 1996). Dyes such as CF, usually applied in diacetate form to promote uptake, have now found widespread use in phloem transport studies. However, none of the above studies had sufficient resolution to examine sieve-element contents during translocation.

Subcellular sieve-tube structures were later imaged by CLSM in leaflets of whole broad bean plants (Knoblauch and van Bel, 1998). As in most other parts of mature plants, the phloem in the main veins is covered by cell layers that prevent a clear view of the sieve-tube components. In the main vein, however, the phloem runs parallel to the surface allowing the removal of cortical layers without injuring sieve tubes (Figure 1d). The phloem was observed through 1–2 remaining parenchyma cell layers that covered the phloem; these did not significantly reduce observation quality but served to protect the sensitive phloem tissue. Distant application of phloem mobile fluorescent dyes proved that observed sieve tubes were translocating. The entire plant was taken to the microscope and the intact leaf mounted on the stage. By employing different fluorescent stains, the *in vivo* location of sieve tube components could be revealed (Figure 1e,f).

In following years, a series of studies were based on this preparation protocol and several important insights on phloem structure and function were achieved (e.g. Furch *et al.*, 2007, 2009). Among them was the discovery of the reversible occlusion of sieve tubes by forisomes. Forisomes are P-protein complexes located in the lumen of sieve tubes of faboid legumes (Figure 2). In response to injury they undergo a calcium-dependent, rapid, reversible conformational change from a spindle shaped low-volume, to a spherical high volume state, thereby occluding the injured sieve tubes (Knoblauch *et al.*, 2001, 2003; Peters *et al.*, 2006, 2007a, 2008, 2010; Thorpe *et al.*, 2010).

The isolation of forisomes and the identification of genes encoding forisome proteins led to the description of the sieve element occlusion (SEO) gene family (Pélissier *et al.*, 2008). Interestingly, although forisomes are restricted to the faboid legumes, sieve element occlusion related genes (SEOR) can be found in other angiosperms including Arabidopsis (Pélissier *et al.*, 2008; Huang *et al.*, 2009; Rüping *et al.*, 2010). AtSEOR1 turned out to be a filamentous sieve-tube protein (Froelich *et al.*, 2011).

For non-invasive, high-resolution imaging of the phloem, small plants such as Arabidopsis remain beneficial. The thin roots are transparent enough to observe the phloem directly. Arabidopsis plants can be grown in glass bottom petri dishes or petri dishes that contain a cover glass for microscopic observation. Microscopy rhizosphere chambers (micro-ROCs) are an alternative with several advantages. In micro-ROCs roots are guided two- dimensionally along a cover glass while the roots are in contact with their natural soil environment. Thus, the root system and plant symbiont/pathogen interactions can be observed throughout the entire life cycle of plants grown under different environmental conditions.

The phloem in roots of AtSEOR1-YFP transgenic plants grown in micro-ROCs was observed at high resolution with the CLSM (Froelich *et al.*, 2011). A distinct fine meshwork of protein filaments and bundles was found in sieve tubes

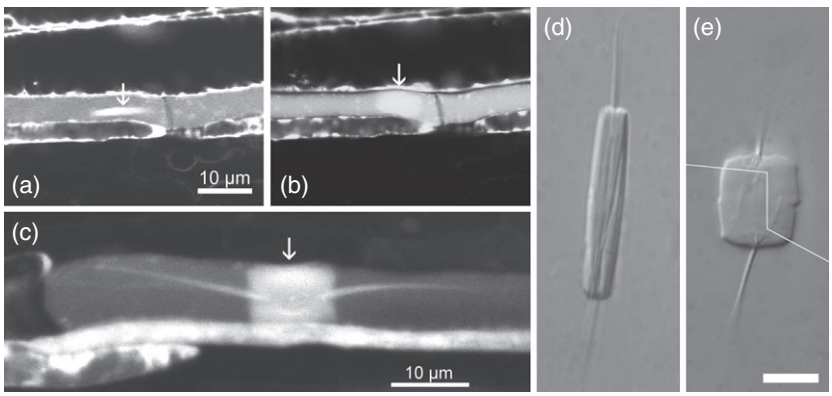

Figure 2. Forisomes *in vivo* and *in vitro*.
(a) Intact sieve tube of Vicia faba contains a forisome (arrow) in the low volume state.
(b) After injury the forisome (arrow) switches into the high volume state and increases resistance in the tube.
(c) A forisome (arrow) of Phaseolus vulgaris in the high volume state. In Phaseolus and many other species forisomes have long extensions called tails. Forisome morphology and distribution is of phylogenetic significance in legumes (Peters *et al.*, 2010).
(d) An isolated forisome of Canavalia gladiata in the low volume (d) and the high volume state (e). Bar = 10 µm. Figures a–c are from Knoblauch *et al.* (2001) with permission of the publisher. Figures d and e are from Peters *et al.* (2007b) with permission of the publisher.

(Figure 3a). These structures had never been seen before and did not match any of the structures found in TEM images to date. Furthermore, large agglomerations of AtSEOR1 proteins, filling the entire lumen of sieve elements, were found frequently (Figure 3b,c).

When CFDA was loaded into the leaves of transgenic AtSEOR1-YFP plants, the dye was translocated throughout the plant and demarcated the actively translocating sieve tubes. Surprisingly, sieve tubes containing large agglomerations of AtSEOR1 proteins translocated equally well as tubes without agglomerations (Froelich *et al.*, 2011), raising questions once gain about the predicted non-occluded nature of translocating sieve tubes.

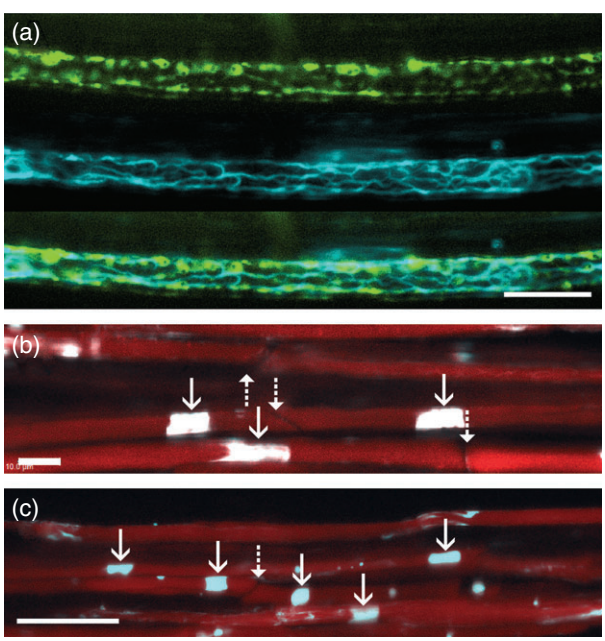

Figure 3. At SEOR1 in Arabidopsis sieve tubes.
(a) At SEOR1-YFP fusion proteins (blue) and GFP tagged to the ER are expressed in stable transgenic Arabidopsis lines. At SEOR1 forms a meshwork of protein filaments covering the margins of the cell. The filaments are often in close contact to the ER.
(b, c) Despite massive AtSEOR1 agglomerations (solid arrows) in the lumen of intact sieve tubes, mass flow is not hindered as indicated by translocation of distantly applied CFDA (red). Sieve plates at dashed arrows. Bars: a, b = 10 µm; c = 40 µm. Figures a–c are from Froelich *et al.* (2011) with permission of the publisher.

Super-resolution microscopy

Recently, significant advances have been made in the field of super-resolution imaging. With respect to plant cells, this subject was reviewed recently by Bell and Oparka (2011) and will not be dealt with in detail here. Briefly, super-resolution imaging approaches offer significant potential with respect to the detailed structure of the phloem, offering significant increases in both lateral (20 nm) and axial (60 nm) resolution (Bell and Oparka, 2011). At present, such techniques are confined largely to immobilized plant samples but rapid advances suggest that real-time imaging at super-resolution is on the horizon. For example, time-lapse Photoactivation Localization Microscopy (PALM) can achieve a temporal resolution of seconds (Biteen *et al.*, 2008) while video-rate Stimulated Emission and Depletion (STED) microscopy has achieved millisecond resolution (Westphal *et al.*, 2008).

In a recent study, Fitzgibbon *et al.* (2010) examined the phloem in tobacco using 3D-structured illumination microscopy (3D-SIM), achieving resolution of individual sieve-plate pores and the pore-plasmodesmata that connect the sieve element with the companion cell (Figure 4). The ability to image protein localization spatially at the level of plasmodesmata offers exciting opportunities for future research on

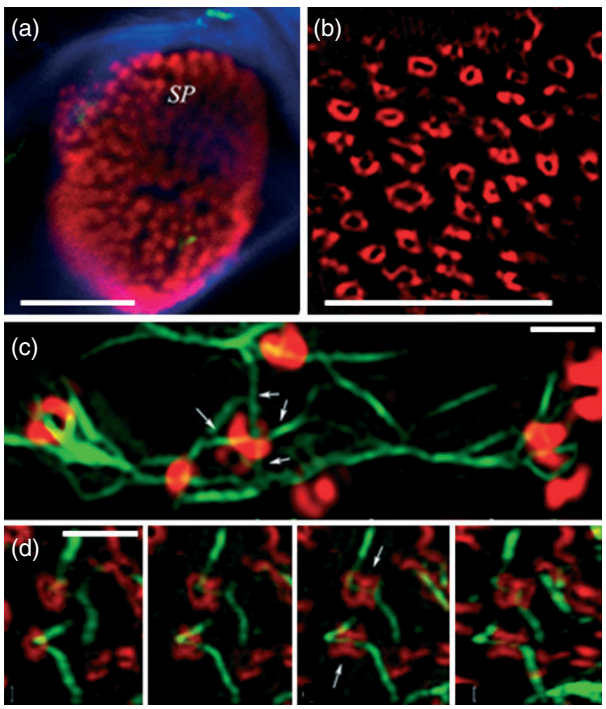

Figure 4. 3D SIM of sieve plates and plasmodesmata.
(a) Mature sieve plate of tobacco stained with antibody to callose (red). Sieve-plate pores are visible but not resolved. Scale = 5 um.
(b) Super-resolution of a sieve plate using 3D-structured illumination microscopy (3D-SIM). Sieve-plate pores, and the callose collars surrounding them, are clearly resolved. Scale = 5 um.
(c) Pore-plasmodesmata connecting sieve element and companion cell are resolved using 3D-SIM. Callose collars (red) associated with individual plasmodesmata are seen, along with fine strands decorated by the movement protein (MP; arrows) of tobacco mosaic virus (green). Scale = 1 um.
(d) Individual sieve-plate pores stained with callose antibody (red) show strands of MP (arrows; green) running through them from one sieve element to another. The images show a rotation series from transverse to loingitudinal views of the pores. Scale = 1 um). Figures c–f are from Fitzgibbon *et al.* (2010) with permission of the publisher.

the location of sieve-element proteins without the need for antibody localization (Fitzgibbon *et al.*, 2010). A future area that is sure to gain importance in the study of the phloem is in the development of CLEM. In this approach, the same biological sample is viewed using a number of approaches sequentially from confocal microscopy, through super-resolution microscopy to transmission electron microscopy, bridging important gaps in image scaling between different instruments. The potential for CLEM with respect to imaging plant cells was reviewed recently by Tilsner and Oparka (2010) and Bell and Oparka (2011).

Transmission electron microscopy (TEM)

The improvement of TEM instrumentation over the last decades has had minimal influence on the overall quality of sieve-tube images. Early work (e.g. that by Cronshaw and Esau, 1968), showed electron micrographs of comparable quality to current images. Whilst atomic resolution is standard in material sciences, the complex 3D structure and the weak interaction of electrons with the atomic nuclei of light elements restricts contrast and resolution. This is the reason why biological samples are stained with heavy metal salts such as uranyl-acetate or lead-citrate. What we finally see in the TEM are not the atoms composing proteins and membranes, but the heavy metal stains. Rather, it has been the improvement and development of preparation protocols for TEM that has advanced our views about sieve-tube structure.

When aldehyde fixatives were developed, sieve tube structure became a focal point and hundreds of papers were published discussing sieve-tube ultrastructure between 1965 and 1980 (for an overview see Behnke and Sjolund, 1990). During this time a surprising variety of structures were described in the lumen of sieve tubes. Since fixation and embedding procedures require small sample sizes, tissue sections were used for TEM, which already contain pre-fixation artifacts. In addition TEM always bears the drawback of fixation and dehydration-induced artifact development. Since the structure of most cellular ingredients is defined by their interaction with water molecules, dehydration may lead to structural alterations. Most electron micrographs showed sieve-tube components such as P-proteins located in the lumen (Figure 5a) and in sieve-plate pores (Figure 5b) of mature sieve elements after standard preparation, resurrecting the arguments that these were dislocation artifacts (Evert *et al.*, 1973; Fisher, 1975; Johnson *et al.*, 1976). Others argued exactly the opposite, claiming that P-proteins in pores were removed due to a preparation-induced surge in images showing open pores (Spanner, 1978). In order to prevent surge-induced artifacts, Evert *et al.* (1973) removed the cotyledons and foliage leaves from the hypocotyl of Cucurbita maxima seedlings. After 2 days they expected the turgor in the sieve tubes to drop significantly due to the lack of photosynthesis, and the tissue was processed by standard procedures for TEM investigation. Electron micrographs showed mostly open pores (Evert *et al.*, 1973). Anderson and Crownshaw (1970) used whole wilted tobacco and bean plants for chemical fixation. The lack of water should have reduced the sieve tube turgor and therefore surge artifacts. The results were inconclusive, since open pores as well as pores with P-protein agglomerations were found in the same samples. Siddiqui and Spanner (1970) showed images of fixed *Helianthus* stems and *Saxifraga* stolons after boiling. The pores were heavily occluded. The same was true when the tissue was fixed after wilting. Other attempts such as freeze substitution (Giaquinta and Geiger, 1973; Fisher, 1975) did not solve the problem of artifact interpretation either. Although significantly more investigators favored open pores as a consequence of the pressure flow hypothesis, the main problem remained that a definitive reference on the location of P-proteins in translocating sieve tubes was lacking. Furthermore, a clear

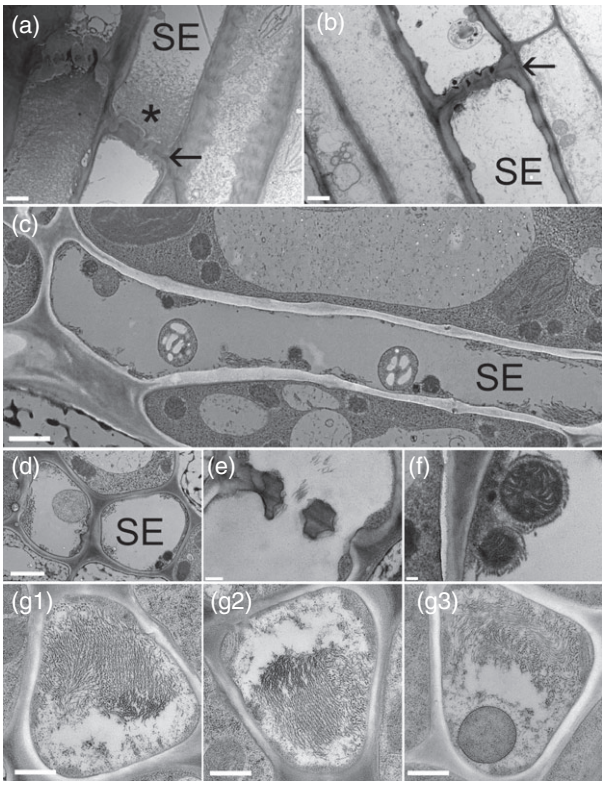

Figure 5. Transmission electron microscopy of sieve tubes.
(a, b) Sieve tubes after standard chemical fixation most often show large plugs (asterisk) of P-protein in front of the sieve plate (a, arrow) or in the lumen and inside sieve plate pores (b).
(c–g) Sieve tube structure after freeze substitution of whole young Arabidopsis plants.
(c) The lumen of the sieve element (SE) is completely free of small filaments as seen in a and b. Instead bundles of filaments are located at the margin of the cell. Sieve element plastids and mitochondria are well preserved.
(d) Cross-section through two sieve tubes. The sieve element (SE) on the right contains bundles of AtSEOR1 filaments and two mitochondria (lower right) at the margins of the cell. The tube to the left also contains large bundles of AtSEOR1 filaments and a sieve element plastid.
(e) Longitudinal section through a sieve plate. Sieve plate pores are unobstructed. The pores do not contain any detectable callose.
(f) Higher magnification of two mitochondria in a sieve tube. Small clamp proteins form a 'halo' around the mitochondria. To which AtSEOR1 filaments are attached.
(g) Three consectutive sections through the lumen of a sieve tube containing AtSEOR1 agglomerations. AtSEOR1 fills almost the entire lumen of the tube. The filaments are well aligned giving an almost crystalline impression in some areas. Figure from Froelich *et al.* (2011) with permission of the publisher. Copyright: American Society of Plant Biologists. Bars a–d = 1 μm; e = 200 nm; f = 100 nm; g = 500 nm.

pressure gradient between the phloem located in source and sink tissues has not been shown experimentally.

Transgenic plants expressing AtSEOR1-YFP fusion proteins finally provided an *in vivo* reference (Froelich *et al.*, 2011). The structure and location of Arabidopsis P-proteins, however, did not match any structures shown in TEM images so far. In order to find a fixation protocol for TEM where the location of P-proteins resembles the location of *in vivo* studies, a number of protocols were tested. The best match was found by plunge freezing whole young plants in nitrogen slush, followed by freeze substitution (Froelich *et al.*, 2011). Sieve tubes processed in this way showed several structures that had not been described before (Figure 5c–f). Surprisingly, both TEM and *in vivo* confocal images showed mostly open pores but often also massive agglomerations of P-protein in translocating sieve tubes (Figures 4 and 5g). The impact of these findings on our understanding of phloem transport is discussed in the proceeding section below.

Scanning electron microscopy (SEM)

In contrast to CLSM and TEM, the impact of SEM on our understanding of sieve tube structure is surprisingly minor. SEM is a powerful tool to examine the surface of materials at high resolution. But because the phloem is embedded in ground tissue, it is usually not accessible with the SEM. In tissue sections that expose the phloem, remnants of the cytoplasm cover structures such as sieve plates, preventing their investigation. Recently, however, Mullendore *et al.* (2010) introduced a preparation protocol to remove the entire protoplast by a consecutive enzymatic digest. Cleared tissue allowed high-resolution imaging and precise measurement of sieve tube geometrical data (Figure 6a–d). The measurements served to estimate frictional interactions of the sap within the tube system and a calculation of the conductivity of sieve tubes.

Magnetic resonance imaging (MRI)

In comparison to the methods described above, MRI has much lower spatial and temporal resolution. The resolution is in general not sufficient to resolve individual sieve tubes and therefore the instruments are not used to generate data on sieve tube structure. However, with regard to the phloem, MRI enables measurement of flow of solutes non-invasively within different tissues. Over the last 15 years, MRI has been used to measure xylem and phloem flow seedlings (Kockenberger *et al.*, 1997), the stem of different dicots (Windt *et al.*, 2006), and the tomato truss stalk (Windt *et al.*, 2009). It has also been employed to study topics such as the diurnal dynamics of long distance transport (Rokitta *et al.*, 1999; Peuke *et al.*, 2001; Windt *et al.*, 2006), the effects of cold girdling (Peuke *et al.*, 2006), and xylem embolism refilling (Scheenen *et al.*, 2001). Mullendore *et al.* (2010) correlated sieve-tube geometry data generated by SEM with MRI flow velocity measurements (Figure 6e–k) and found that lower resistance of the tube does not lead to higher flow velocities. Instead an inverse relation was found.

IMPACT OF HIGH-RESOLUTION IMAGING AND MEASUREMENT ON OUR UNDERSTANDING OF PHLOEM TRANSPORT

The investigations over the last decades have shown beyond doubt that there is mass flow in sieve tubes. However, it

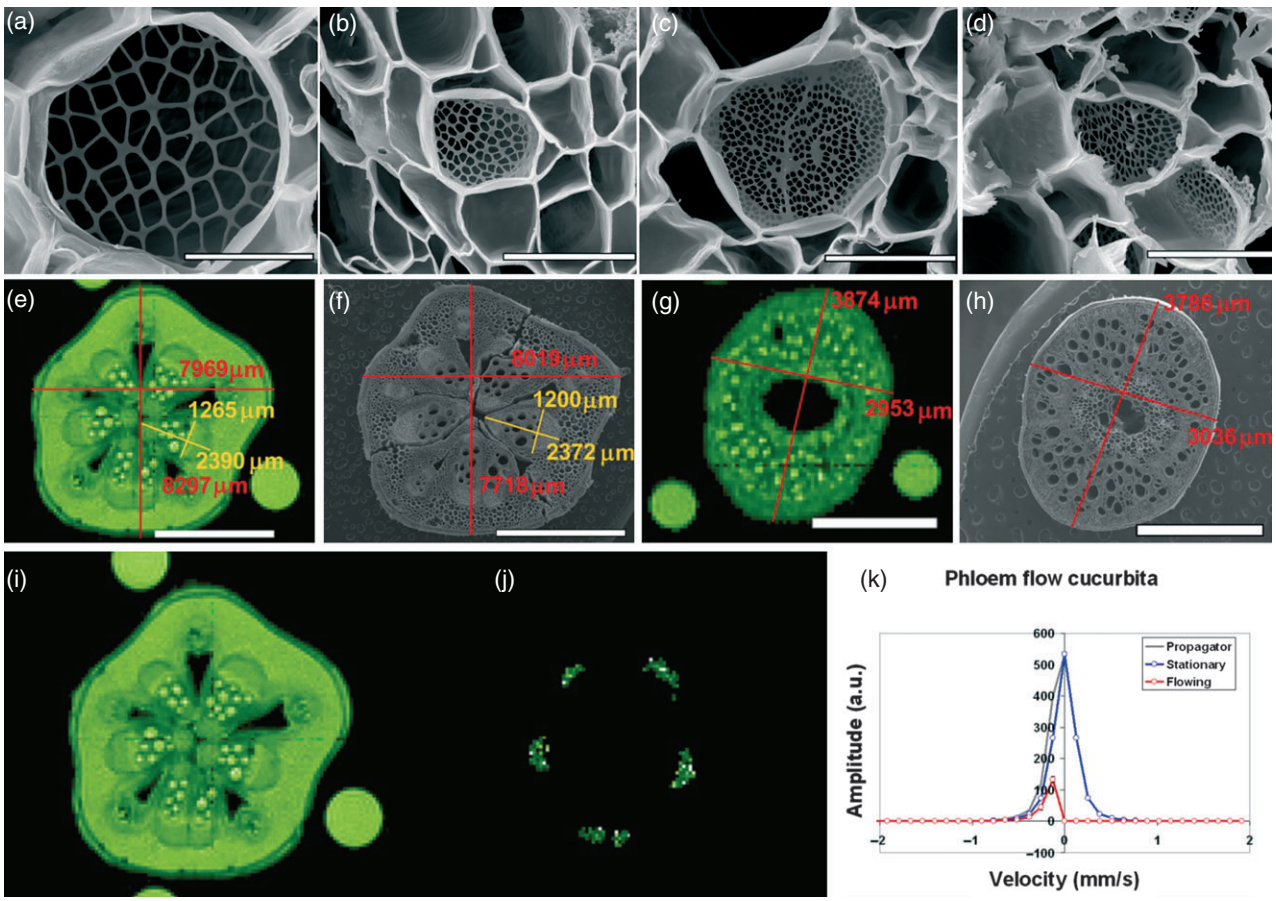

Figure 6. Scanning electron microscopy (SEM) of sieve plates and MRI flow velocimetry.
(a–d) SEM of sieve plates after removal of the protoplast. Sieve plates of Cucurbita maxima (a), Phaseolus vulgaris (b), Rhicinus communis (c), and Solanum lycopersicum (d), at the same magnification.
(e) MRI and (f) SEM images of Cucurbita maxima and Phaseolus vulgaris (g, h) stems. MRI images were taken in intact plants. Preparation for SEM does not lead to significant geometrical alterations as indicated by the measurements in e–h.
(i) Amplitude (i.e., water content) maps of Cucurbita were acquired from a T1 inversion recovery measurement and serve as an anatomical reference for the phloem flow velocity maps (j). The cumulative velocity profile (total propagator) for all phloem sap flow containing pixels was constructed (k). Making use of the fact that the flow profile of stationary water is symmetrical around zero, the diffusing but stationary water in the flow mask (red) was separated from the flowing water (blue). Bars: a–d = 20 µm, e–h = 2 mm. Figure from Mullendore *et al.* (2010) with permission of the publisher.

remains unclear as to whether a pressure gradient along the sieve tubes is the driving force. Besides the general geometry of the tube system, it is important to know the viscosity and velocity of the sap flowing through the tube in order to model flow. Velocity can be measured by MRI, carbon isotopes and fluorescence-based methods (Jensen *et al.*, 2011), and viscosity can be derived from sugar, amino acid and ion concentrations of phloem sap collected from severed aphid stylets (Deeken *et al.*, 2002; Hunt *et al.*, 2009). Based on geometrical, viscosity, and velocity data, it was concluded that (at least in large trees) the phloem might be organized in relays; that is in tubes shorter than the plant's axial length, with loading and unloading between them. This is because the pressure required to drive flow would exceed the value that can be generated in source sieve tubes (Lang, 1979; Thompson and Holbrook, 2003). In addition, the turgor pressure in sieve tubes does not scale with plant size. Small herbaceous plants often have much higher turgor pressures than trees (Turgeon, 2010). Recently, however, Jensen *et al.* (2011) reported that they found a scaling relation of radius r and the characteristic lengths as $r = (L_{leaf}\ L_{stem})^{1/3}$ for optimization of translocation speed. Flow velocity measurements and biomimicking microfluidic devices support this scaling relation and provide the first quantitative support for a unified mechanism of sugar translocation in plants spanning several orders of magnitude in size.

SO WHY IS THERE STILL A PROBLEM?

Contrary to expectation, recent high-resolution non-invasive studies of the phloem have not provided unequivocal support for the Münch pressure-flow hypothesis. This is an uncomfortable situation given its widespread acceptance.

The observation that there is an inverse relation between conductivity and flow velocity in sieve tubes (Mullendore *et al.*, 2010) may suggest that the volume to surface area ratio is critical for flow velocity. Since wider tubes have a lower surface area ratio, uptake and unloading capacity of assimilates and water through sieve tube membranes may define flow velocity (Thompson, 2006; Jensen *et al.*, 2011).

New, non-invasive approaches depict the sieve tube as a very dynamic system with large agglomerations of SEOR proteins in Arabidopsis, apparently blocking individual sieve elements. Yet, the flow of low-molecular weight dyes of the same size as a sucrose molecule is unimpeded through these protein masses (Froelich *et al.*, 2011), which suggests that a pressure flow is possible despite obstructions in the pathway. This is a surprising fact because observation of P-protein agglomerations were regarded as contrary to a pressure flow and led to alternative theories some decades ago. In the future it will be important to test the porosity and size exclusion limit of the protein material. Those data need to be included into flow models. It will also be crucial to obtain more information on the occurrence and location of P-proteins in living sieve tubes of different species. A crucial problem is, however, the lack of data on the presence of a pressure differential between source and sink. A central tenet of the pressure-flow hypothesis is that flow is driven by a hydrostatic pressure gradient along the tube. Precise geometrical data in combination with pressure differential measurements would finally provide the basis to confirm or refute Münch's hypothesis. Regarding sieve-tube structure, current instrumentation developments will help to solve open questions. Super-resolution methods hold much promise with respect to the phloem. Because of extended image acquisition times these methods are currently limited to immobilized samples, but it is likely that technical improvements will soon allow dynamic live-cell imaging at resolutions down to 20 nm (Bell and Oparka, 2011).

During its development the sieve element undergoes a remarkable autolysis in which some organelles are lost while others are retained. It can be likened to a highly selective programmed cell death that is without parallel amongst plant cells. What is the role of the different organelles that are retained within sieve elements? Older studies regarded these as vestigial structures (reviewed in Esau, 1969). However, recent studies suggest the sieve element periphery, or 'parietal layer' may carry out several functions. For example, the mature sieve element houses several of the enzymes involved in alkaloid biosynthesis (Bird *et al.*, 2003), while mature sieve-element plastids contain enzymes of jasmonate biosynthesis (Hause *et al.*, 2003). The mature sieve element lacks a classical secretory system yet retains an elaborate ER network, indicating that further attention is merited on the mechanisms of protein trafficking between companion cells and sieve elements via the specialized pore-plasmodesmata that connect these cells (Bell and Oparka, 2011). Finally, the sieve-element plasma membrane contains a plethora of pumps, channels and proteins that must constantly be turned over in this enucleate cell and yet we know little of its membrane composition. It seems likely that the phloem will continue to baffle and delight researchers for several decades to come. New advances in imaging are likely to play a continuing role in elucidating the structure and function of the sieve element.

ACKNOWLEDGEMENTS

We thank Jessica Fitzgibbon and Karen Bell for critical reading of the manuscript. Work in Michael Knoblauch's lab is supported by NSF grant no 1022106. Work in the Oparka laboratory is funded by the BBSRC.

REFERENCES

Anderson, R. and Crownshaw, J. (1970) Sieve-plate pores in tobacco and bean. *Planta*, **91**, 173–180.

Barclay, G.F., Oparka, K.J. and Johnson, R.P.C. (1977) Induced disruption of sieve element plastids in *Heracleum mantagazzianum* L. *J. Exp. Bot.* **28**, 709–717.

Behnke, H.D. and Sjolund, R.D. (1990) *Sieve Elements*. Berlin: Springer.

Bell, K. and Oparka, K. (2011) Imaging plasmodesmata. *Protoplasma*, **248**, 9–25.

Bird, D.A., Franceschi, V.R. and Facchini, P.J. (2003) A tale of three cell types: alkaloid biosynthesis is localized to sieve elements in opium poppy. *Plant Cell*, **15**, 2626–2635.

Biteen, J.S., Thompson, M.A., Tselentis, N.K., Bowman, G.R., Shapiro, L. and Moerner, W.E. (2008) Super-resolution imaging in live *Caulobacter crescentus* cells using photoswitchable EYFP. *Nat. Methods*, **5**, 947–949.

Canny, M.J.P. (1975). Mass transfer. In *Encyclopedia of Plant Physiology*, Vol. 1 (Zimmermann, M.H. and Milburn, J.A., eds). Berlin: Springer, pp. 139–153.

Cronshaw, J. and Esau, K. (1968) P-protein in the phloem of Cucurbita. II. The P-protein of mature sieve elements. *J. Cell Biol.* **38**, 292–303.

Deeken, R., Geiger, D., Fromm, J., Koroleva, O., Ache, P., Langenfeld-Heyser, R., Sauer, N., May, S. and Hedrich, R. (2002) Loss of the AKT2/3 potassium channel affects sugar loading into the phloem of *Arabidopsis*. *Planta*, **216**, 334–344.

Esau, K. (1969). The phloem. Encyclopedia of Plant Anatomy IX. Gebruder Borntraeger.

Esau, K. and Cheadle, V.I. (1959) Size of pores and their contents in sieve elements of dicotyledons. *PNAS*, **45**, 156–162.

Evert, R.F., Eschrich, W. and Eichhorn, S.E. (1973) P protein distribution in mature sieve elements of *Cucurbita maxima*. *Planta*, **109**, 193–210.

Fensom, D.S. (1957) The bioelectric potentials of plants and their functional significance. I. An electrokinetic theory of transport. *Can. J. Bot.* **35**, 573–582.

Fisher, D.B. (1975) Structure of functional soybean sieve elements. *Plant Physiol.* **56**, 555–569.

Fitzgibbon, J., Bell, K., King, E. and Oparka, K.J. (2010) Super-resolution imaging of plasmodesmata using three-dimensional structured illumination microscopy. *Plant Physiol.* **153**, 1453–1463.

Froelich, D.F., Mullendore, D.L., Jensen, K.H., Ross-Elliott, T.J., Anstead, J.A., Thompson, G.A., Pelissier, H.C. and Knoblauch, M. (2011) Phloem ultrastructure and pressure flow: SEOR protein agglomerations do not affect translocation. *Plant Cell*, **23**, 4428–4445.

Furch, A.C.U., Hafke, J.B., Schulz, A. and van Bel, A.J.E. (2007) Ca2+- mediated remote control of reversible sieve tube occlusion in *Vicia faba*. *J. Exp. Bot.* **58**, 2827–2838.

Furch, A.C.U., van Bel, A.J.E., Fricker, M.D., Felle, H.H., Fuchs, M. and Hafke, J.B. (2009) Sieve element Ca2+ channels as relay stations between remote stimuli and sieve tube occlusion in *Vicia faba*. *Plant Cell*, **21**, 2118–2132.

Giaquinta, R.T. and Geiger, D.R. (1973) Mechanism of inhibition of translocation by localized chilling. *Plant Physiol.* **51**, 372–377.

Grignon, N., Touraine, B. and Durand, M. (1989) 6(5) carboxyfluorescein as a tracer of phloem sap translocation. *Am. J. Bot.* **76**, 871–877.

Hartig, T. (1854) Über die Querscheidewände zwischen den einzelnen Gliedern der Siebröhren in *Cucurbita pepo*. *Bot. Z.* **12**, 51–54.

Hause, B., Hause, G., Kutter, C., Miersch, O. and Wasternack, C. (2003) Enzymes of jasmonate biosynthesis occur in tomato sieve elements. *Plant Cell Physiol.* **44**, 643–648.

Huang, S., Li, R., Zhang, Z. *et al.* (2009) The genome of the cucumber, *Cucumis sativus* L. *Nat. Genet.* **41**, 1275–1281.

Hunt, E., Gattolin, S., Newbury, H.J., Bale, J.S., Tseng, H.-M., Barrett, D.A. and Pritchard, J. (2009) A mutation in amino acid permease AAP6 reduces the amino acid content of the *Arabidopsis* sieve elements but leaves aphid herbivores unaffected. *J. Exp. Bot.* **61**, 55–64.

Jensen, K.H., Lee, J., Bohr, T., Bruus, H., Holbrook, N.M. and Zwieniecki, M.A. (2011). Optimality of the Münch mechanism for translocation of sugars in plants. *J. R. Soc. Interface*, **8**, 1155–1165.

Johnson, R.P.C., Freundlich, A. and Barclay, G.F. (1976) Transcellular strands in sieve tubes; What are they? *J. Exp. Bot.* **101**, 1117–1136.

Knoblauch, M. and Peters, W.S. (2010) Münch, morphology, microfluidics – our structural problem with the phloem. *Plant Cell Environ.* **33**, 1439–1452.

Knoblauch, M. and van Bel, A.J.E. (1998) Sieve tubes in action. *Plant Cell*, **10**, 35–50.

Knoblauch, M., Peters, W.S., Ehlers, K. and van Bel, A.J.E. (2001) Reversible Calcium-Regulated Stopcocks in Legume Sieve Tubes. *Plant Cell*, **13**, 1221–1230.

Knoblauch, M., Noll, G.A., Müller, T., Prüfer, D., Schneider-Hüther, I., Scharner, D., van Bel, A.J.E. and Peters, W.S. (2003) ATP-independent contractile proteins from plants. *Nat. Mater.* **2**, 600–603.

Kockenberger, W., Pope, J.M., Xia, Y., Jeffrey, K.R., Komor, E. and Callaghan, P.T. (1997) A non-invasive measurement of phloem and xylem water flow in castor bean seedlings by nuclear magnetic resonance microimaging. *Planta*, **201**, 53–63.

Lang, A. (1979) A relay mechanism for phloem translocation. *Ann. Bot. (Lond.)*, **44**, 141–145.

Mullendore, D.L., Windt, C.W., van As, H. and Knoblauch, M. (2010) Sieve tube geometry in relation to phloem flow. *Plant Cell*, **22**, 579–593.

Münch, E. (1927) Versuche über den Saftkreislauf. *Ber. Dtsch. Bot. Ges.* **45**, 340–356.

Münch, E. (1930) *Die Stoffbewegungen in der Pflanze*. Gustav Fischer: Jena.

Oparka, K.J. and Turgeon, R. (1999) Sieve elements and companion cells – traffic control centers of the phloem. *Plant Cell*, **11**, 739–750.

Oparka, K.J., Duckett, C.M., Prior, D.A.M. and Fisher, D.B. (1994) Real-time imaging of phloem unloading in the root tip of *Arabidopsis*. *Plant J.* **6**, 759–766.

Pélissier, H.C., Peters, W.S., Collier, R., van Bel, A.J.E. and Knoblauch, M. (2008) GFP-tagging of sieve element occlusion (SEO) proteins results in green fluorescent forisomes. *Plant Cell Physiol.* **49**, 1699–1710.

Peters, W.S., van Bel, A.J. and Knoblauch, M. (2006) The geometry of the forisome-sieve element-sieve plate complex in the phloem of *Vicia faba* L. leaflets. *J. Exp. Bot.* **57**, 3091–3098.

Peters, W.S., Schnetter, R. and Knoblauch, M. (2007a) Reversible birefringence suggests a role for molecular self-assembly in forisome contractility. *Funct. Plant Biol.* **34**, 302–306.

Peters, W.S., Knoblauch, M., Warman, S.A., Schnetter, R., Shen, A.Q. and Pickard, W.F. (2007b) Tailed forisomes of Canavalia gladiate: a new model to study Ca2+ – driven protein contractility. *Ann. Bot.* **100**, 101–109.

Peters, W.S., Knoblauch, M., Warmann, S.A., Pickard, W.F. and Shen, A.Q. (2008) Anisotropic contraction in forisomes: simple models won't fit. *Cell Motil. Cytoskel.* **65**, 368–378.

Peters, W.S., Haffer, D., Hanakam, C.B., Van Bel, A.J.E. and Knoblauch, M. (2010) Legume phylogeny and the evolution of a unique contractile protein apparatus that regulates phloem transport. *Am. J. Bot.* **97**, 797–808.

Peuke, A.D., Rokitta, M., Zimmermann, U., Schreiber, L. and Haase, A. (2001) Simultaneous measurement of water flow velocity and solute transport in xylem and phloem of adult plants of Ricinus communis over a daily time course by nuclear magnetic resonance spectrometry. *Plant Cell Environ.* **24**, 491–503.

Peuke, A.D., Windt, C. and Van As, H. (2006) Effects of cold-girdling on flows in the transport phloem in Ricinus communis: is mass flow inhibited? *Plant Cell Environ.* **29**, 15–25.

Rokitta, M., Peuke, A.D., Zimmermann, U. and Haase, A. (1999) Dynamic studies of phloem and xylem flow in fully differentiated plants by fast nuclear-magnetic-resonance microimaging. *Protoplasma*, **209**, 126–131.

Rüping, B., Ernst, A., Jekat, S., Nordzieke, S., Reineke, A., Müller, B., Bornberg-Bauer, E., Prüfer, D. and Noll, G. (2010) Molecular and phylogenetic characterization of the sieve element occlusion gene family in *Fabaceae* and non-*Fabaceae* plants. *BMC Plant Biol.* **10**, 219.

Scheenen, T.W., Vergeldt, F.J., Windt, C.W., de Jager, P.A. and Van As, H. (2001) Microscopic imaging of slow flow and diffusion: a pulsed field gradient stimulated echo sequence combined with turbo spin echo imaging. *J. Magn. Reson.* **151**, 94–100.

Schulz, A. (1992) Living sieve cells of conifers as visualized by confocal, laser-scanning fluorescence microscopy. *Protoplasma*, **166**, 153–164.

Siddiqui, A.W. and Spanner, D.C. (1970) The state of the pores in functioning sieve plates. *Planta*, **91**, 181–189.

Spanner, D.C. (1958) The translocation of sugar in sieve tubes. *J. Exp. Bot.* **9**, 332–342.

Spanner, D.C. (1970) The electroosmotic theory of phloem transport in the light of recent measurements of *Heracleum* phloem. *J. Exp. Bot.* **21**, 325–334.

Spanner, D.C. (1978) Sieve-plate pores, open or occluded? A critical review. *Plant Cell Environ.* **1**, 7–20.

Thaine, R. (1961) Transcellular strands and particle movement in mature sieve tubes. *Nature*, **192**, 772–773.

Thaine, R. (1962) A translocation hypothesis based on the structure of plant cytoplasm. *J. Exp. Bot.* **13**, 152–160.

Thaine, R. (1969) Movement of sugars through plants by cytoplasmic pumping. *Nature*, **222**, 873–875.

Thompson, M.V. (2005) Scaling phloem transport: elasticity and pressure-concentration waves. *J. Theor. Biol.* **236**, 229–241.

Thompson, M.V. (2006) Phloem: the long and the short of it. *Trends Plant Sci.* **11**, 26–32.

Thompson, M.V. and Holbrook, N.M. (2003) Application of a singlesolute non-steady-state phloem model to the study of longdistance assimilate transport. *J. Theor. Biol.* **220**, 419–455.

Thorpe, M.R., Furch, A.C.U., Minchin, P.E.H., Föller, J., van Bel, A.J.E. and Hafke, J.B. (2010) Rapid cooling triggers forisome dispersion just before phloem transport stops. *Plant Cell Environ.* **33**, 259–271.

Tilsner, J. and Oparka, K.J. (2010) Tracking the green invaders: advances in imaging virus infection in plants. *Biochem. J.* **430**, 21–37.

Turgeon, R. (2010) The Puzzle of Phloem Pressure. *Plant Physiol.* **154**, 578–581.

Van Bel, A.J.E. and Knoblauch, M. (2000) Sieve element and companion cell: the story of the comatose patient and the hyperactive nurse. *Aust. J. Plant Physiol.* **27**, 477–487.

Westphal, V., Rizzoli, S.O., Lauterbach, M.A., Kamin, D., Jahn, R. and Hell, S.W. (2008) Video-rate far-field optical nanoscopy dissects synaptic vesicle movement. *Science*, **320**, 246–249.

Windt, C.W., Vergeldt, F.J., De Jager, P.A. and Van As, H. (2006) MRI of long-distance water transport: a comparison of the phloem and xylem flow characteristics and dynamics in poplar, castor bean, tomato and tobacco. *Plant Cell Environ.* **29**, 1715–1729.

Windt, C.W., Gerkema, E. and Van As, H. (2009) Most water in the tomato truss is imported through the xylem, not the phloem: a nuclear magnetic resonance flow imaging study. *Plant Physiol.* **151**, 830–842.

Wright, K.M. and Oparka, K.J. (1994) Physicochemical properties alone do not predict the movement and compartmentation of fluorescent xenobiotics. *J. Exp. Bot.* **45**, 35–44.

Wright, K.M. and Oparka, K.J. (1996) The use of HPTS as a symplastic, phloem-mobile tracer: an evaluation using confocal laser scanning microscopy. *J. Exp. Bot.* **47**, 439–445.

Wright, K.M., Horobin, R.W. and Oparka, K.J. (1996) Phloem mobility of fluorescent xenobiotics in *Arabidopsis* in relation to their physicochemical properties. *J. Exp. Bot.* **47**, 1779–1787.